Halogen-Free Ciamician-Dennstedt Single-Atom Skeletal Editing

Xihe Bi

bixh507@nenu.edu.cn

Northeast Normal University https://orcid.org/0000-0002-6694-6742

Shaopeng Liu

Northeast Normal University

Yong Yang

Northeast Normal University

Qingmin Song

Northeast Normal University

Zhaohong Liu

Northeast Normal University https://orcid.org/0000-0001-9951-8675

Paramasivam Sivaguru

Northeast Normal University https://orcid.org/0000-0003-2225-0054

Yifan Zhang

Northeast Normal University

Graham Ruiter

Schulich Faculty of Chemistry, Technion - Israel Institute of Technology

Edward Anderson

University of Oxford https://orcid.org/0000-0002-4149-0494

Article

Keywords:

Posted Date: June 18th, 2024

DOI: https://doi.org/10.21203/rs.3.rs-4163086/v1

Additional Declarations: There is **NO** Competing Interest.

Version of Record: A version of this preprint was published at Nature Communications on November 19th, 2024. See the published version at https://doi.org/10.1038/s41467-024-54379-8.

Abstract

Single-atom skeletal editing is an increasingly powerful tool for scaffold hopping-based drug discovery. However, the insertion of a single functionalized carbon atom into heteroarenes remains exceedingly rare, especially when performed in complex chemical settings, due to the challenge of overcoming aromaticity without uncontrolled degradation. For example, the Ciamician–Dennstedt rearrangement, in which a carbene is inserted into an indole or pyrrole ring, remains limited to halocarbene precursors despite more than a century of research. Herein, we report a general methodology for the halogen-free Ciamician-Dennstedt reaction, which enables the direct conversion of indoles/pyrroles into structurally diverse quinoline/pyridine scaffolds. The generality and applicability of this methodology were demonstrated by extensive scope investigation and product derivatizations, as well as by concise syntheses and late-stage skeletal editing of complex bioactive compounds. Mechanistic studies reveal a pathway that involves the intermediacy of a 1,4-dihydroquinoline intermediate, which could undergo oxidative aromatization or defluorinative aromatization to form different carbon-atom insertion products.

Introduction

The concept of “scaffold-hopping”, which aims to identify isofunctional structures with distinct molecular cores that enhance bioactivity and also access new intellectual property space, has recently emerged as an important, enabling strategy in drug discovery[1,2]. One of the most desirable contexts of this powerful concept is heterocycle replacement, as showcased by the successful development of the cholesterol-lowering drug pitavastatin from fluvastatin, and the antineoplastic agent alimta from and 5,10-dideazafolic acid (Fig. 1a)[3,4]. However, the execution of this strategy in molecular optimization campaigns has proven to be time-consuming and labour-intensive due to the often-distinct preparative methods required for the different heterocyclic cores. As such, synthetic and medicinal chemists are particularly attracted to direct heterocycle-to-heterocycle transmutation by the insertion or deletion of single-atoms from the heterocyclic core of a given active pharmaceutical ingredient[5–8]. Within this field, significant advances have been made in single-atom skeletal editing of aliphatic heterocycles, presumably due to the relative ease of activation and manipulation of these frameworks[9–17]. However, the execution of this concept in the setting of heteroaromatic scaffolds is far more challenging[19–26], owing to the high energy barriers encountered during the initial dearomatization processes required for single-atom insertion, which in turn can impose limitations on the range of insertion reagents, or reaction conditions[26,27].

One of the seminal examples of the single-atom skeletal editing is the Ciamician–Dennstedt (C-D) reaction, in which pyrroles are converted into 3-chloropyridines via the formal insertion of chloroform-derived dichlorocarbene[28]. Unfortunately, despite over a century of study, this transformation has seen limited applications due to its harsh reaction conditions and poor yields that can result from competing Reimer-Tiemann formylation[29,30]. Recent years have seen important contributions to the evolution of this chemistry, most notably by the groups of Levin, Ball, and others[31–35]. Mechanistically, these C-D

reactions proceed via initial carbene formation and halocyclopropanation of the heterocycle, followed by aromatization-promoted 2π-electrocyclic ring opening with concurrent loss of the halide leaving group. Indeed, the expulsion of this halide ion in the course of ring expansion is critical to ensure selective C–C bond cleavage (by electrocyclic ring opening) over C–H functionalization (by cyclopropane fragmentation). Consequently, only specially-designed halocarbene precursors, such as chloroform[28], CCl_3CO_2Na[30], chlorodiazirine[31,32], halodiazoacetates[33,34], and dibromofluoromethane[35] have been successfully deployed in these one-carbon insertions. In spite of these advances, the application of C-D reactions in late-stage skeletal modifications of complex targets therefore remains highly challenging and relatively underdeveloped due to the limited functional group compatibility of the intermediate carbenes (and the associated reaction conditions), as well as the restricted pool of potential halocarbene precursors[30–35].

A mechanistically distinct yet general approach that does not rely on halide ion expulsion, and could thus utilize a halogen-free carbene precursor, would propel this important skeletal editing technique to a prime position within the synthetic organic chemistry arsenal, and unlock the Ciamician-Dennstedt reaction for the broad, late-stage editing of pharmaceuticals (Fig. 1c). Here we report the successful implementation of a general and broadly applicable halogen-free C-D reaction of indoles and pyrroles to access 3-functionalized quinolines and pyridines. Critical to this transformation is a mechanistically distinct pathway, enabled by the use of functionalized *N*-triftosylhydrazones as carbene precursors, and driven by a thermodynamically-favored oxidative aromatization process. *N*-triftosylhydrazones are structurally diverse, and can be readily prepared from a wide variety of commercially available and naturally occurring carbonyl compounds[17,25,36–39]. Due to this structural diversity, this halogen-free C-D reaction enables the direct introduction of a wide range of carbon sidechains, with indoles and pyrroles converted into 3-trifluoromethyl, 3-difluoromethyl, 3-fluoroalkyl, 3-formyl, 3-aryl, 3-alkenyl and 3-alkynyl substituted quinolines and pyridines, which are well-known, privileged structural elements in drug and agrochemical development[40,41]. This operationally safe protocol is highly chemoselective and features excellent functional group compatibility, rendering it operable in complex settings, as demonstrated by concise syntheses of bioactive molecules possessing quinoline ring systems and the late-stage modification of indole-containing natural products.

Results and Discussion

Given the prominence of fluoroalkyl groups in drug and agrochemical development[42, 43], we first directed our attention to the insertion of fluoroalkylated carbon atoms into indoles, which would offer facile access to 3-fluoroalkylated quinolines. After optimization of various reaction parameters (See Tables S1 and S2), we found that the reaction of *N*-TBS-indole **1** with trifluoroacetaldehyde *N*-triftosylhydrazone (TFHZ-Tfs, **2**)[44] in the presence of NaH and the copper(I) catalyst $Tp^{Br3}Cu(NCMe)$ (10 mol%), followed by *in situ* treatment of the intermediate cyclopropane **3'** with TBAF and DDQ, directly afforded 3-(trifluoromethyl)quinoline **3** in 86% yield.

We next explored the scope of this one-pot, two-step skeletal ring expansion reaction of indoles with fluoroalkyl *N*-triftosylhydrazones. As shown in Fig. 2a, a range of *N*-TBS-indoles bearing electron-donating or electron-withdrawing substituents at the 4-, 5-, 6-, or 7-positions afforded the corresponding 3-trifluoromethyl quinoline products in good to excellent yields (5–22). Many functional groups, such as methyl (5–8), ester (9), acetyl (10), halogens (11, 18, 19, 21, and 22), ethers (12, 16, and 20), amine (13), phenyl (14), pyridine (15), and phenylethynyl (17) were well tolerated, although electron-donating substituents afforded slightly reduced yields of the 3-trifluoromethylated quinolines (e.g., **5–8**, **12**, **13**, and **20**). In contrast to this moderate electronic influence, steric factors can play a crucial role in the reaction; for example, 3-methyl-TBS-indole produced ring expansion product **4** in ~ 20% yield. Nonetheless, the extensive functional group compatibility, combined with the mild reaction conditions, offers much potential for the late-stage modification of complex molecules of biological relevance: for instance, a bioactive natural product, raputimonoindole B, as well as indoles derived from naturally occurring terpenes geraniol and perillyl alcohol, underwent smooth insertion to afford their corresponding quinoline homologs (23–25). In addition to trifluoroacetaldehyde *N*-triftosylhydrazone (TFHZ-Tfs), difluoroacetaldehyde *N*-triftosylhydrazone (DFHZ-Tfs)[45] could also be used in our ring expansion protocol, affording 3-difluoromethylated quinolines (26–33) in high yields and with excellent chemoselectivity. Aside from indoles, the reaction of 7-azaindole with TFHZ-Tfs or DFHZ-Tfs also performed well to afford the corresponding ring expansion products **34** and **35**.

We then investigated the reactivity of longer chain fluoroalkyl *N*-triftosylhydrazones. Under the standard conditions, the reaction of *N*-TBS-indole with pentafluoroethyl *N*-triftosylhydrazone produced the expected ring expansion product **36** in 60% yield along with small amounts (20%) of a hydrodefluorinative ring expansion product **37**. Intrigued by the formation of **37**, we re-optimized the reaction conditions to favor the formation of this hydrodefluorination product, which no longer required the addition of the oxidant DDQ (see Table S4); gratifyingly, we obtained **37** in 98% yield in the presence of caesium fluoride (CsF) in H_2O/DMSO under air at 25 °C. As shown in Fig. 2b, a wide variety of structurally diverse indoles with functionalities such as halogen, ester, ether, amine, methyl, alkynyl, and allyloxy substituents readily underwent this modified ring-expansion reaction, affording 3-fluoroalkylated quinoline products (38–48) in moderate to good yields, and could be extended to an azaindole (49). We found that longer-chain perfluoroalkyl *N*-triftosylhydrazones were also compatible with the transformation, producing the corresponding functionalized carbon-atom insertion products (**50–55**) in high yields, in which the fluorine atom at the α-carbon of the hydrazone chain has undergone selective defluorination.

Surprisingly, we found that the outcome of this reaction could be further tuned by treatment of the cyclopropane intermediate (**3'**) under identical conditions (CsF/H_2O/DMSO under air), but at 40 °C instead of 25°C, which led to the formation of quinoline-3-carboxaldehyde (**56**) in 78% yield (Table S6). This unexpected defluorinative formylation affords a formal carbonylative insertion product, and turned out to be quite general, with a wide array of electronically differentiated indoles proving compatible with these reaction conditions. In all cases the corresponding quinoline-3-carboxaldehyde products (**57–67**)

were obtained in high yields. Remarkably, indoles derived from naturally occurring terpenes such as geraniol and perillyl alcohol were also transformed smoothly into their corresponding quinoline-3-carboxaldehyde analogs **68** and **69** respectively, in spite of their potentially vulnerable ester and alkene functionalities, demonstrating the potential of our protocol for the late-stage modification of chemically-complex indole-containing bioactive molecules.

We recognized that the value of this chemistry would be significantly enhanced if other hydrazones could be applied, and turned our attention to the synthesis of 3-arylquinolines using aryl and heteroaryl aldehyde-derived *N*-triftosylhydrazones as carbene precursors. While the reaction of *N*-TBS-indole with 4-tolyl *N*-triftosylhydrazone under the previously optimized conditions delivered the desired ring expansion product **70** in only 20% yield, after significant re-optimization we were delighted to discover that $Tp^{Br3}Ag(THF)$ improved this yield to 97% (Fig. 3a, see Table S6 for details). Under these new conditions, a wide variety of electronically differentiated aryl *N*-triftosylhydrazones were successfully inserted, with tolerance of functionalities such as phenyl, naphthyl, trifluoromethyl, trifluoromethoxy, halogens, and ethers (**71**–**80**). The practicality of our protocol was demonstrated by the gram-scale synthesis of **70**. The extension of this method to *N*-triftosylhydrazones bearing a fused or hetero aromatic ring would be of great significance for drug discovery. We found that this indeed proved possible, with furan, benzofuran, benzothiophene, thiophene, and pyridine substituents all successfully introduced in high yields in the ring expansion to products (**81**–**86**). We could further expand the scope of *N*-triftosylhydrazone substitutents to alkyl, alkene, and even alkyne groups; these insertions also proceeded smoothly, producing the corresponding 3-alkyl-, alkenyl-, and alkynyl-quinolines (**87**–**92**) in good to excellent yields. The incorporation of these unsaturated moieties provides valuable functional handles for additional downstream synthetic transformations.

Having established the broad scope of the *N*-triftosylhydrazone partner that can be employed in this chemistry, we turned our attention to the indole substrate. To our delight, using 4-tolyl *N*-triftosylhydrazone as the carbene precursor, indoles adorned with bromo, nitro, ester, pyridine, allyloxy, hydroxy, amine, phenyl, halogen, methoxy, cyano, and acetal functionalities at any of the positions on the indole scaffold proved successful, affording the corresponding 3-arylquinolines (**93–106**) in moderate to excellent yields. Particularly notable is the successful insertion of sterically challenged 2,3-dimethyl- and 4-fluoro-5-OTBS-2-methyl-substituted indoles, which gave respectable yields of quinolines **107** and **108**. Interestingly, OTBS (*tert*-butyldimethylsilyloxy) group can be tolerated in the first step, but is hydrolysed to hydroxyl in the second step, which provides a practical route to access hydroxyl-containing bioactive compounds (*vide infra*). In addition, 7-azaindole and 5-chloro-7-azaindole also delivered the corresponding ring expansion products (**109** and **110**). We also demonstrated the applicability of this silver-catalyzed protocol to the late-stage modification of bioactive indoles through the successful ring-expansion of tryptophol, melatonin, raputimonoindole B, and verticillatine B, which provided the respective ring-expansion products **111**–**114** in moderate yields. Key drug intermediates (e.g., pindolol), or indoles derived from steroids (e.g., pregnenolone) or terpenes (e.g., perillyl alcohol and geraniol) also proved good substrates, affording their 3-aryl quinoline analogs **115–118**.

Of high importance in molecular editing is the ability to apply a single reaction to multiple heterocyclic cores. As such, we next addressed the application of our protocol to the transmutation of pyrrole into pyridine. Although *N*-TBS-protected pyrroles failed to provide the targeted cyclopropanation product using phenyl *N*-triftosylhydrazone, reaction of 1*H*-pyrrole, using $Rh_2(esp)_2$ as catalyst, afforded the ring expanded pyridine **119** in 48% yield (see Table S7). With suitable modified editing conditions established, we first investigated the range of *N*-triftosylhydrazone coupling partners that could be used. As shown in Fig. 3b, we found that a variety of mono- and di-substituted aryl *N*-triftosylhydrazones bearing trifluoromethyl, fluoro, ester, methyl, and chloro substituents directly afforded the corresponding 3-aryl pyridines (**120–125**). A brief survey of pyrrole scope revealed that 2-(trichloroacetyl)-1*H*-pyrrole provided the desired pyridine **126** in 59% yield, while 3-methyl-1*H*-pyrrole resulted in a 4:3 mixture of regioisomeric ring expansion products **127** and **128**, in 56% yield.

To further demonstrate the utility of the ring-editing protocol, we targeted the streamlined syntheses of a number of bioactive quinolines of medicinal interest (Fig. 4). 3-Aryl quinolines are common motifs in such compounds, however their construction typically requires multiple steps for the synthesis and functionalization of the quinoline ring, which can limit development. Our methodology, on the other hand, is simple, easy to implement, and generally results in high yields of 3-aryl quinolines by direct transmutation of more readily-available indoles. For example, we successfully synthesized potential anticancer agents compounds **130** and **131** from indole **129** in a single step, in 77% and 53% yield respectively. Previous approaches required three step protocols starting from 3-methoxyaniline, which proceeded with overall yields of 3.3% (**130**) and 9.2% (**131**)[46], clearly demonstrating the efficiency of our ring expansion protocol. Similarly, we were able to prepare quinoline **133**, which is used for the treatment of hypopharyngeal cancer, in two steps from indole **132** with 70% overall yield via C-D insertion followed by Buchwald-Hartwig amination with morpholine. Previous routes employed 1,2-difluoro-4-nitrobenzene as starting material, and gave **133** in 47% overall yield via a five step protocol[47]. The efficiency of preparation of the antimycobacterial treatment adjuvant **134**, previously prepared via a five-step synthetic protocol with an overall yield of 20%[48], could be nearly doubled by employing the C-D insertion (overall yield 37%) while reducing the number of synthetic steps. Moreover, 3-arylquinoline-2-carboxaldehyde **137**, a key intermediate for the synthesis of pharmaceuticals with antiproliferative activity (**138)** and anti-dengue activity (**139**), was previously obtained from isatin in three steps with 53% total yield[49]. However, using the herein developed methodology, compound **137** can be accessed in two steps from 2-methylindole **134** in 62% overall yield. Subsequently, compound **137** could be readily converted into **138** by a Claisen-Schmidt condensation or to compound **139** *via* a Cannizzaro reaction. Finally, this silver-catalyzed one-carbon insertion could also be used for *de novo* syntheses of anti-inflammatory compound **140**[50] in four steps with 38% overall yield from indole **134**, and β-glucuronidase inhibitor **142**[51] in three steps with 40% overall yield from indole **141**.

Mechanistic investigations

To gain insight into the mechanism of the halogen-free C-D reaction, we performed a series of experiments to study the reaction pathway for the formation of the various products (Fig. 5). First, trifluoromethyl cyclopropane **144** was isolated as a single diastereomer on reaction of indole **143** with TFHZ-Tfs (2) (Fig. 5a). Treatement of **144** with CsF in dry DMSO under a nitrogen atmosphere at room temperature for 10 minutes gave a mixture of **145** and **146** in a ~ 1:1 ratio (82%). Subjection of these products to additional CsF and water, under air at 40°C, resulted in the formation of formal formylation product **62** in 80% yield. This suggests that 1,4-dihydroquinoline **145** or 3,4-dihydroquinoline **146** are both key intermediates in the formation of the aldehyde product. Further, resubjection 3-(difluoromethyl)quinoline **29** to the same conditions did not afford any aldehyde **62**, ruling out the possibility of difluoromethyl hydrolysis to the aldehyde.

We next performed a series of deuterium labeling studies (Fig. 5b). Treatment of deuterated cyclopropanated indole **147-d** with TBAF in D_2O resulted in the formation of the bis-deuterated 1,4-dihydroquinoline **148-d$_2$** (80% D incorporation). Reaction of **148-d$_2$** under the standard conditions (CsF / H_2O, DMSO, air, 40°C) afforded **56-d** with 74% D incorporation at the carbonyl carbon and 85% D retention at the C4-position. In contrast, reaction of the mono-deuterated 1,4-dihydroquinoline **148-d$_1$** (99% D) afforded **56-d** with 23% D incorporation at the carbonyl carbon and 75% D retention at the C4-position, indicating a kinetic isotope effect (k_H/k_D) of 3:1. These experiments demonstrate that the aldehyde hydrogen of **56** is derived from the C4-position of the 1,4-dihydroquinoline intermediate, and appear to suggest an internal 1,3-hydride shift, which may be the rate-determining step of the reaction. Interestingly, treatment of deuterated cyclopropane **149-d** with TBAF in THF at 25°C under a nitrogen atmosphere afforded the deuterated quinoline **150** in 98% yield, with 40% D incorporation at the N1-position and 30% D incorporation at the C4-position, which indicated an imine-enamine tautomerization process. Susequently, **150** could be oxidized (by air), giving rise to 3-arylquinoline **70-d** in 97% yield and with 10% D retention at the C4-position, suggesting that the direct carbon-insetion may proceed through an oxidative dehydrogenation of 1,4-dihydroquinoline. Finally, subjection of trifluoromethyl cyclopropane **147** to the standard reaction conditions, but with $H_2{}^{18}O$ instead of H_2O, produced the ^{18}O-incorporated quinoline-3-carboxaldehyde **56-^{18}O**, showing that the oxygen atom in the aldehyde is derived from water (Fig. 5c).

Based on these experiments, possible reaction pathways for the C-D editing of indoles with fluoroalkyl carbenes is shown in Fig. 5d. First, [2 + 1] cycloaddition of the indole with the *in situ* generated fluoroalkyl carbene generates the *N*-TBS protected cyclopropane intermediate **I**, which undergoes deprotection under the influence of TBAF or CsF. Concurrent or subsequent ring-opening yields the 3,4-dihydroquinoline anion **II**, which is protonated (by water) to furnish the 1,4-dihydroquinoline intermediate **IV** after imine-enamine tautomerization. From this key intermediate, two pathways are possible, depending on the reaction conditions. Firstly, intermediate **IV** (R = F) can undergo oxidative aromatization mediated by the strong oxidant DDQ to produce the 3-(trifluoromethyl)quinoline (3) (pathway I). Alternatively, the *gem*-difluoromethylene intermediate **V** can be generated via a base-mediated elimination of fluoride (pathway II). As evidenced by the deuterium labeling studies (*vide supra*),

intermediate **V** (R = perfluoroalkyl group) undergoes a 1,3-hydride shift to deliver the defluorinated product **37**. However, for intermediate **V** (R = F), oxa-Michael addition of water occurs to form intermediate **VI**, followed by HF elimination to generate intermediate **VII**. From **VII**, a 1,3-hydride shift occurs to produce an intermediate **VIII**, which eliminates another molecule of HF to furnish the quinoline-3-carboxaldehyde product **56**.

To further support this proposed mechanism shown in Fig. 5d, we performed a computational study of the ring-opening of cyclopropane intermediate **Int1**. Nucleophilic attack of fluoride on the TBS group in **Int1**, via transition state **TS1** ($\Delta G^{\ddagger}$ = 15.2 kcal/mol), generates the zwitterionic intermediate **Int3**, which is exergonic by 28.3 kcal/mol (from **Int-1**) providing the thermodynamic driving force for the ring-opening (Fig. 6a). Protonation of **Int3** with H_2O via transition state **TS2** ($\Delta G^{\ddagger}$ = 7.8 kcal/mol) results in imine intermediate **Int5**, which can isomerize to the more stable enamine **Int6** with a free energy release of ΔG^{0} = -3.6 kcal/mol. The formation of **Int6** from **Int4** is reversible. These calculated mechanism for ring-opening of **Int1** are fully supported by our deuterium labelling studies on the ring-opening of deuterium-labeled cyclopropane **149** to afford the N1 and C3 deuterium labeled intermediate **150** (Fig. 5b). The 1,4-dihydroquinoline **Int6** then undergoes a CsF-mediated 1,4-elimination of fluoride via **TS3** to generate the *gem*-difluoromethylene intermediate **Int8** with a modest barrier of 13.0 kcal/mol (Fig. 6a). The relatively low barrier is due to the F•••Cs interaction as well as C–H•••O and C–H•••F hydrogen bond interactions between the solvent and the indole that stabilizes transition state **TS3**, which results in facile elimination of HF. This facile formation of the *gem*-difluoromethylene is also supported by our experimental results (Fig. 5b). Subsequently, a 1,4-oxa-Michael addition of H_2O to the *gem*-difluoromethylene **Int-8** affords intermediate **Int10** with an energy barrier of 6.2 kcal/mol (Fig. 6b). In turn, **Int10** must overcome a relatively large energy barrier of 22.4 kcal/mol (via **TS5**) to eliminate CsF and subsequently form the enol intermediate **Int11**. A CsF/DMSO assisted 1,3-H shift via **TS6** ($\Delta G^{\ddagger}$ = 24.3 kcal/mol) produces **Int12**, which is the rate-determining step in the reaction. This calculated rate-determining step is in line with the experimental observation that C–H bond cleavage is involved in the rate limiting step (supported by its kinetic isotope effect, Fig. 5b). Finally, elimination of HF from **Int12** furnishes the quinoline-3-carboxaldehyde product **56**. The elimination of HF in the final step is assisted by CsF, lowering the barrier to $\Delta G^{\ddagger}$ = 5.7 kcal/mol (Fig. 6b).

We also investigated computationally the origin of the difference in reaction outcomes between the CF_3- and C_2F_5-substituted carbenes, via analysis of the key transition states that lead to defluorinative formylation insertion product **56** and hydrodefluorination insertion product **37** (Fig. 6c). Our calculations show that **Int8** – generated from the CF_3-substituted carbene – strongly prefers the Michael addition of H_2O (via **TS4**, $\Delta G^{\ddagger}$ = 6.2 kcal/mol) over CsF-assisted 1,3-H transfer that leads to defluorinative product **26** (via **TS4'**, $\Delta G^{\ddagger}$ = 18.1 kcal/mol) (Fig. 6c). The preference of the Michael addition over the 1,3-H shift is consistent with our experimental findings that 3-(difluoromethyl)quinoline **26** failed to give any of carbonylation product **56** under the standard conditions (Fig. S17). By contrast, for **Int8-1** – generated from the C_2F_5-substituted carbene – opposite chemoselectivity is observed. For **Int8-1**, the 1,3-H transfer

is significantly preferred over the Michael addition reaction (compare **TS4-1'**: $\Delta G^{\ddagger}$ = 1.2 kcal/mol vs. **TS4-1**: $\Delta G^{\ddagger}$ = 7.2 kcal/mol). The origin of this reversed selectivity appears to derive from the difference in electronegativity between O and C atoms in **TS4** (Δe = 2.005), which is larger than that in **TS4-1** (Δe = 1.489). The large difference in electronegativity is due to the strong electron-withdrawing effect of the trifluoromethyl group compared to the fluorine atom, which also explains the relatively lower activation barrier of **TS4** (Fig. S18). In addition, conformational analysis indicates that the energy barrier for the 1,3-H transfer may be influenced by the conformational change between the transition state and its precursor. More specifically, the electrostatic repulsion between the fluorine and oxygen atoms in transition state **TS4-1'** is stronger than those in **TS4'**, making the change in conformation between **TS4-1'** and its precursor **Int8-1** smaller than that between **TS4'** and **Int8** (Fig. S18).

Taken together, our combined experimental and DFT calculation results indicate that the formal carbon-atom insertion proceeds through a cyclopropanation/fragmentation cascade to generate a key 1,4-dihydroquinoline intermediate, which can undergo an unprecedented defluorinative aromatization to deliver the hydrodefluorination insertion product **37** or the defluorinative carbonylation insertion product **56**, depending on the carbene precursor and reaction conditions. In both processes, CsF and DMSO play critical roles in controlling the chemoselectivity and lowering the activation energy through transition state stabilization via hydrogen bonding interactions.

Conclusion

The use of *N*-triftosylhydrazones as carbene precursors has enabled the first halogen-free Ciamician-Dennstedt reaction, provide a method for the direct editing of indoles and pyrroles by insertion of a wide range of functionalized carbon atoms. This chemistry accesses diverse libraries of 3-substituted quinoline and pyridine scaffolds. Distinct from the classical C-D reaction pathway, this insertion reaction proceeds either through (i) an oxidative aromatization or (ii) a defluorinative aromatization of the 1,4-dihydroquinoline intermediate, including an unprecedented defluorinative formylation of the trifluoromethyl group. The methodology is general, straightforward, scalable, and is compatible with a wide variety of functional groups, making it applicable for the late-stage skeletal modification of highly-functionalized *N*-heteroarenes. Given the increasing importance of scaffold hopping in medicinal chemistry, we anticipate widespread application in the late-stage synthesis and skeletal modification of functionalized *N*-heteroarenes, with consequent benefits in drug design.

Declarations

Data availability

The data that support the findings of this study are available within the paper and its Supplementary Information.

Acknowledgements

This work was financially supported by the National Natural Science Foundation of China (No. 22331004 to X.B. and No. 22371035 to Z.L.) and the Department of Science and Technology of Jilin Province (No. 20230508054RC and 20240305092YY to Z.L.). E.A. and X.B. thank the Royal Society for support (Newton Advanced Fellowship to X.B., NAF\R1\191210).

Author contributions

S.L., Y.Y., and Q.S. contributed equally to this work.S.L. and Y.Y. conducted the experiments and analyzed the data. Q.S. carried out the DFT calculations. Y.Z. helped with substrate synthesis and data collection. G.R. provided NHC-Fe/Co catalysts. Z.L., E.A., and X.B. conceived the concept, supervised the experiments, and prepared the manuscript with P.S. and G.R. All authors discussed the results and commented on the manuscript.

Competing interests

The authors declare no competing interests.

Supplementary information

The online version contains supplementary material available at https://doi.org

Correspondence and requests for materials should be addressed to Z.L., E.A., and X.B.

References

1. Hu, Y., Stumpfe, D. & Bajorath, J. Recent advances in scaffold hopping. *J. Med. Chem.***60**, 1238–1246 (2017).
2. Acharya, A., Yadav, M., Nagpure, M., Kumaresan, S. & Guchhait, S. K. Molecular medicinal insights into scaffold hopping-based drug discovery success. *Drug Discov. Today***19**, 103845 (2024).
3. Endo, A. A historical perspective on the discovery of statins. *Proc. Jpn. Acad. Ser. B Phys. Biol. Sci.***86**, 484–493 (2010).
4. Taylor, E. C. in *Successful Drug Discovery*, Fischer, J. D. & Rotella, P. Eds. (Wiley 2015), pp. 157–180.
5. Jurczyk, J. *et al.* Single-atom logic for heterocycle editing. *Nat. Synth.***1**, 352–364 (2022).
6. Peplow, M. 'Almost magical': chemists can now move single atoms in and out of a molecule's core. *Nature***618**, 21–24 (2023).
7. Liu, Z., Sivaguru, P., Ning, Y., Wu, Y. & Bi, X. Skeletal editing of (hetero)arenes using carbenes. *Chem. Eur. J.***29**, e202301227 (2023).
8. Joynson, B. W. & Ball, L. T. Skeletal editing: interconversion of arenes and heteroarenes. *Helv. Chim. Acta***106**, e202200182 (2023).
9. Roque, J. B., Kuroda, Y., Göttemann, L. T., & Sarpong, R. Deconstructive diversification of cyclic amines. *Nature***564**, 244–248 (2018).

10. Jurczyk, J. *et al.* Photomediated ring contraction of saturated heterocycles. *Science***373**, 1004–1012 (2021).
11. Lyu, H., Kevlishvili, I., Yu, X., Liu, P. & Dong, G. Boron insertion into alkyl ether bonds via zinc/nickel tandem catalysis. *Science***372**, 175–182 (2021).
12. Kennedy, S. H., Dherange, B. D., Berger, K. J. & Levin, M. D. Skeletal editing through direct nitrogen deletion of secondary amines. *Nature***593**, 223–227 (2021).
13. Hui, C., Brieger, L., Strohmann, C. & Antonchick, A. P. Stereoselective synthesis of cyclobutanes by contraction of pyrrolidines. *J. Am. Chem. Soc.***143**, 18864–18870 (2021).
14. Miller, D. C., Lal, R. G., Marchetti, L. A. & Arnold, F. H. Biocatalytic one-carbon ring expansion of aziridines to azetidines via a highly enantioselective [1,2]-stevens rearrangement. *J. Am. Chem. Soc.* **144**, 4739–4745 (2022).
15. Wright, B. A. *et al.* Skeletal editing approach to bridge-functionalized bicyclo[1.1.1]pentanes from azabicyclo[2.1.1]hexanes. *J. Am. Chem. Soc.* **145**, 10960–10966 (2023).
16. Zhong, H. *et al.* Skeletal metalation of lactams through a carbonyl-to-nickel-exchange logic. *Nat. Commun.***14**, 5273 (2023).
17. Ning, Y., Chen, H., Ning, Y., Zhang, J. & Bi, X. Rhodium-catalyzed one-carbon ring expansion of aziridines with vinyl-*N*-triftosylhydrazones for the synthesis of 2-vinyl azetidines. *Angew. Chem. Int. Ed.***63**, e202318072 (2024).
18. Reisenbauer, J. C., Green, O., Franchino, A., Finkelstein, P. & Morandi, B. Late-stage diversification of indole skeletons through nitrogen atom insertion. *Science***377**, 1104–1109 (2022).
19. Woo, J. *et al*. Scaffold hopping by net photochemical carbon deletion of azaarenes. *Science***376**, 527–532 (2022).
20. Wang, H. J. *et al*. Dearomative ring expansion of thiophenes by bicyclobutane insertion. *Science***381**, 75–81 (2023).
21. Hyland, E. E., Kelly, P. Q., McKillop, A. M., Dherange, B. D. & Levin, M. D. Unified access to pyrimidines and quinazolines enabled by N–N cleaving carbon atom insertion. *J. Am. Chem. Soc.***144**, 19258–19264 (2022).
22. Huang, X.-Y., Xie, P.-P., Zou, L.-M., Zheng, C. & You, S.-L. Asymmetric dearomatization of indoles with azodicarboxylates via cascade electrophilic amination/aza-prins cyclization/phenonium-like rearrangement. *J. Am. Chem. Soc.***145**, 11745–11753 (2023).
23. Bartholomew, G. L., Carpaneto, F. & Sarpong, R. Skeletal editing of pyrimidines to pyrazoles by formal carbon deletion. *J. Am. Chem. Soc.***144**, 22309–22315 (2022).
24. Boudry, E., Bourdreux, F., Marrot, J., Moreau, X. & Ghiazza, C. Dearomatization of pyridines: photochemical skeletal enlargement for the synthesis of 1,2-diazepines. *J. Am. Chem. Soc.***146**, 2845–2854 (2024).
25. Li, L. *et al.* Dearomative insertion of fluoroalkyl carbenes into azoles leading to fluoroalkyl heterocycles with a quaternary center. *Angew. Chem. Int. Ed.***63**, e202313807 (2024).

26. Cheng, Q. *et al.* Skeletal editing of pyridines through atom-pair swap from CN to CC. *Nat. Chem.* (2024). https://doi.org/10.1038/s41557-023-01428-2.
27. Sattler, A. & Parkin, G. Cleaving carbon–carbon bonds by inserting tungsten into unstrained aromatic rings. *Nature***463**, 523–526 (2010).
28. Ciamician, G. L. & Dennstedt, M. Ueber die einwirkung des chloroforms auf die kaliumverbindung pyrrols. *Ber. Dtsch. Chem. Ges.* **14**, 1153–1163 (1881).
29. Wynberg, H. The Reimer-Tiemann Reaction. *Chem. Rev.***60**, 169–184 (1960).
30. Ma, D., Martin, B. S., Gallagher, K. S., Saito, T. & Dai, M. One-carbon insertion and polarity inversion enabled a pyrrole strategy to the total syntheses of pyridine-containing *Lycopodium* alkaloids: Complanadine A and Lycodine. *J. Am. Chem. Soc.***143**, 16383–16387 (2021).
31. Dherange, B. D., Kelly, P. Q., Liles, J. P., Sigman, M. S. & Levin, M. D. Carbon atom insertion into pyrroles and indoles promoted by chlorodiazirines. *J. Am. Chem. Soc.* **143**, 11337–11344 (2021).
32. Joynson, B. W., Cumming, G. R. & Ball, L. T. Photochemically mediated ring expansion of indoles and pyrroles with chlorodiazirines: synthetic methodology and thermal hazard assessment. *Angew. Chem. Int. Ed.***62**, e20231419 (2023).
33. Mortén, M., Hennum, M. & Bonge-Hansen, T. Synthesis of quinoline-3-carboxylates by a Rh(II)-catalyzed cyclopropanation-ring expansion reaction of indoles with halodiazoacetates. *Beilstein J. Org. Chem.***11**, 1944–1949 (2015).
34. Stenner, R., Steventon, J. W., Seddon, A. & Anderson, J. L. R. A de novo peroxidase is also a promiscuous yet stereoselective carbene transferase. *Proc. Natl. Acad. Sci. USA***117**, 1419–1428 (2020).
35. Guo, H., Qiu, S. & Xu, P. One-carbon ring expansion of indoles and pyrroles: a straightforward access to 3-fluorinated quinolines and pyridines. *Angew. Chem. Int. Ed.***64**, e202317104 (2023).
36. Liu, Z., Sivaguru, P., Zanoni, G. & Bi, X. *N*-Triftosylhydrazones: a new chapter for diazo-based carbene chemistry. *Acc. Chem. Res.***55**, 1763–1781 (2022).
37. Liu, S. *et al.* Tunable molecular editing of indoles with fluoroalkyl carbenes. *Nat. Chem.* (2024). https://doi.org/10.1038/s41557-024-01468-2
38. Liu, Z. *et al.* Site-selective C–H benzylation of alkanes with *N*-triftosylhydrazones leading to alkyl aromatics. *Chem***6**, 2110–2114 (2020).
39. Yang, Y. *et al.* Site-selective C–H allylation of alkanes: facile access to allylic quaternary sp^3-carbon centers. *Angew. Chem. Int. Ed.***62**, e202214519 (2023).
40. Michael, J. P. Quinoline, quinazoline and acridonealkaloids. *Nat. Prod. Rep.***25**, 166–187 (2008).
41. Heravi, M. M. & Zadsirjan, V. Prescribed drugs containing nitrogen heterocycles: an overview. *RSC Adv.* **10**, 44247–44311 (2020).
42. Wang, J. *et al.* Fluorine in pharmaceutical industry: fluorine-containing drugs introduced to the market in the last decade (2001–2011). *Chem. Rev.* **114**, 2432–2506 (2014).

43. Zhou, Y. *et al.* Next generation of fluorine-containing pharmaceuticals, compounds currently in phase II–III clinical trials of major pharmaceutical companies: new structural trends and therapeutic areas. *Chem. Rev.***116**, 422–518 (2016).
44. Zhang, X. *et al.* Use of trifluoroacetaldehyde *N*-tfsylhydrazone as a trifluorodiazoethane surrogate and its synthetic applications. *Nat. Commun.***10**, 284 (2019).
45. Ning, Y. *et al.* Difluoroacetaldehyde *N*-triftosylhydrazone (DFHZ-Tfs) as a bench-stable crystalline diazo surrogate for diazoacetaldehyde and difluorodiazoethane. *Angew. Chem. Int. Ed.***59**, 6473–6481 (2020).
46. Hu, Y. *et al.* Antitumor and topoisomerase ⅡΑ inhibitory activities of 3-aryl-7-hydroxyquinolines. *Chin. J. Org. Chem.***39**, 3230–3236 (2019).
47. Thandra, D. R. & Allikayala, R. Synthesis, characterization, molecular structure determination by single crystal X-ray diffraction, and Hirshfeld surface analysis of 7-fluoro-6-morpholino-3-phenylquinolin-1-ium chloride salt and computational studies of its cation. *J. Mol. Struct.***1250**, 131701 (2022).
48. Felicetti, T. *et al.* Modifications on C6 and C7 positions of 3-phenylquinolone efflux pump inhibitors led to potent and safe antimycobacterial treatment adjuvants. *ACS Infect. Dis.***5**, 982–1000 (2019).
49. Tseng, C.-H. *et al.* Synthesis and antiproliferative evaluation of 3-phenylquinolinylchalcone derivatives against non-small cell lung cancers and breast cancers. *Eur. J. Med. Chem.***59**, 274–282 (2013).
50. Yang, C.-Y. *et al.* Discovery of 2-substituted 3-arylquinoline derivatives as potential anti-Inflammatory agents through inhibition of LPS-induced inflammatory responses in macrophages. *Molecules***24**, 1162 (2019).
51. Cheng, K.-W. *et al.* Specific inhibition of bacterial *β*-glucuronidase by pyrazolo[4,3-c]quinoline derivatives via a pH-dependent manner to suppress chemotherapy-induced intestinal toxicity. *J. Med. Chem.***60**, 9222–9238 (2017).

Figures

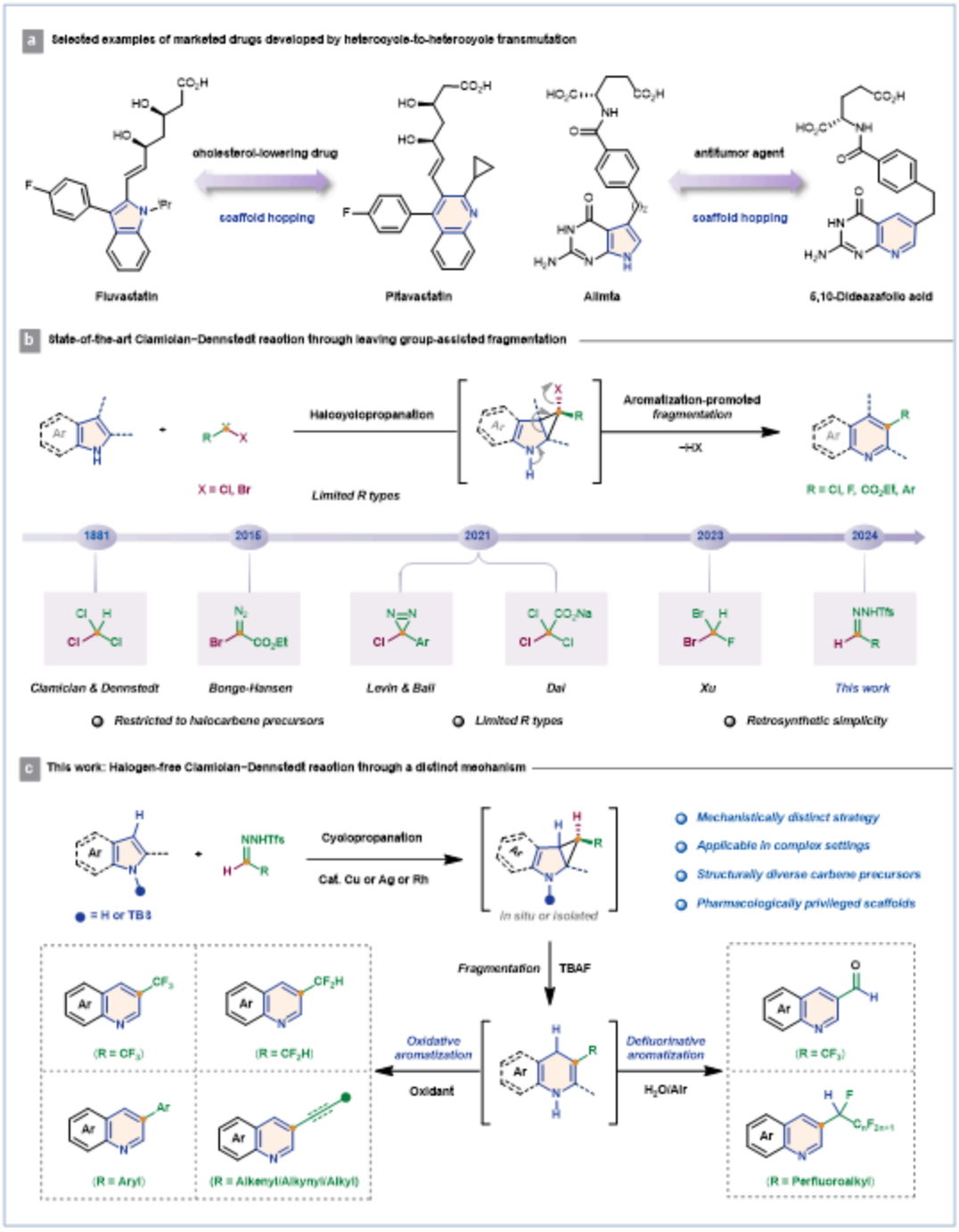

Figure 1

Ciamician-Dennstedt rearrangement reaction: background and development. **a,** The significance of heterocycle-to-heterocycle transmutation in successful drug discovery. **b,** State-of-the-art methods for Ciamician-Dennstedt reaction. **c,** This work: halogen-free Ciamician-Dennstedt reaction through a mechanistically distinct approach. Cat. [M] = $Tp^{Br3}Cu(MeNC)$, $Tp^{Br3}Ag(THF)$ or $Rh_2(esp)_2$.

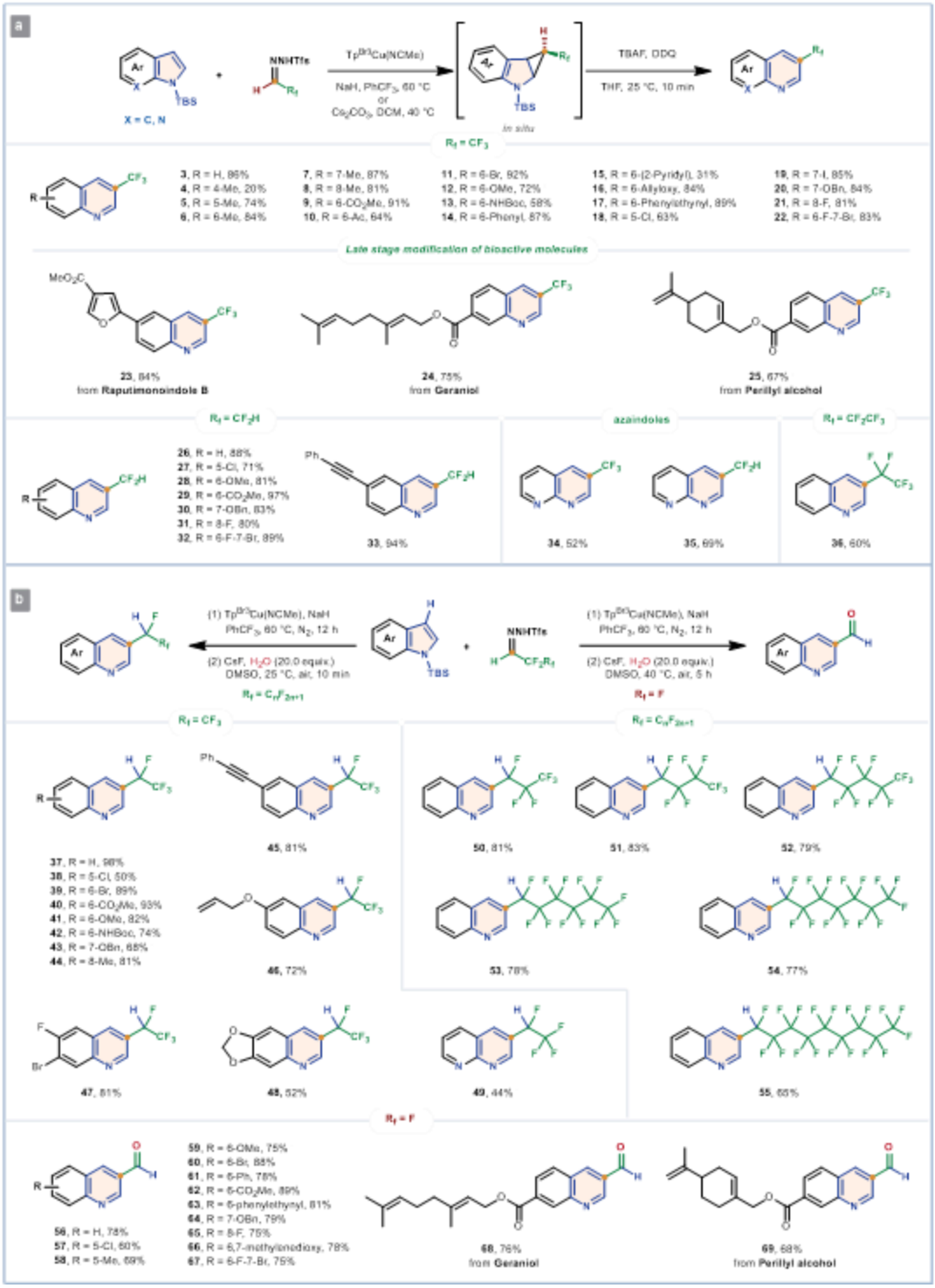

Figure 2

Skeletal ring-expansion of indoles with fluoroalkyl *N*-triftosylhydrazones. a, Direct carbon-atom insertion of indoles with fluoroalkyl carbenes. **b,** Hydrodefluorinative and defluorinative formylation carbon-atom insertion of indoles with fluoroalkyl carbenes. Reactions performed on a 0.3 mmol scale. Isolated yields. See supplementary imformation for details.

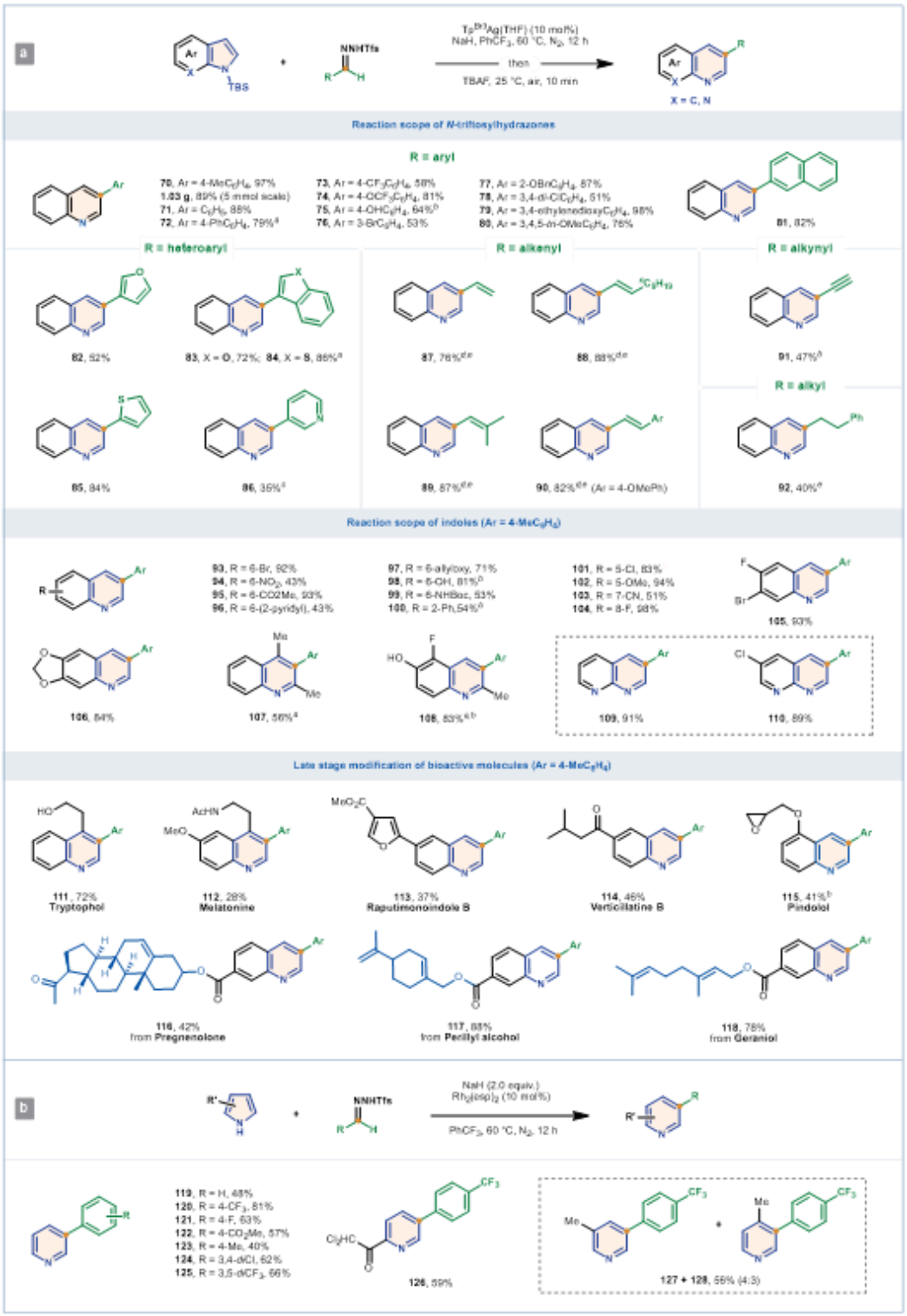

Figure 3

Skeletal ring-expansion of (a) indoles / (b) pyrroles with functionalized *N*-triftosylhydrazones. Reactions performed on a 0.3 mmol scale. Isolated yields. See supplementary materials for details. [a]80 °C. [b]CsF/DMSO instead of TBAF. [c]DCM instead of $PhCF_3$. [d]CsF/DMF instead of TBAF. [e]1 mol % $Rh_2(esp)_2$.

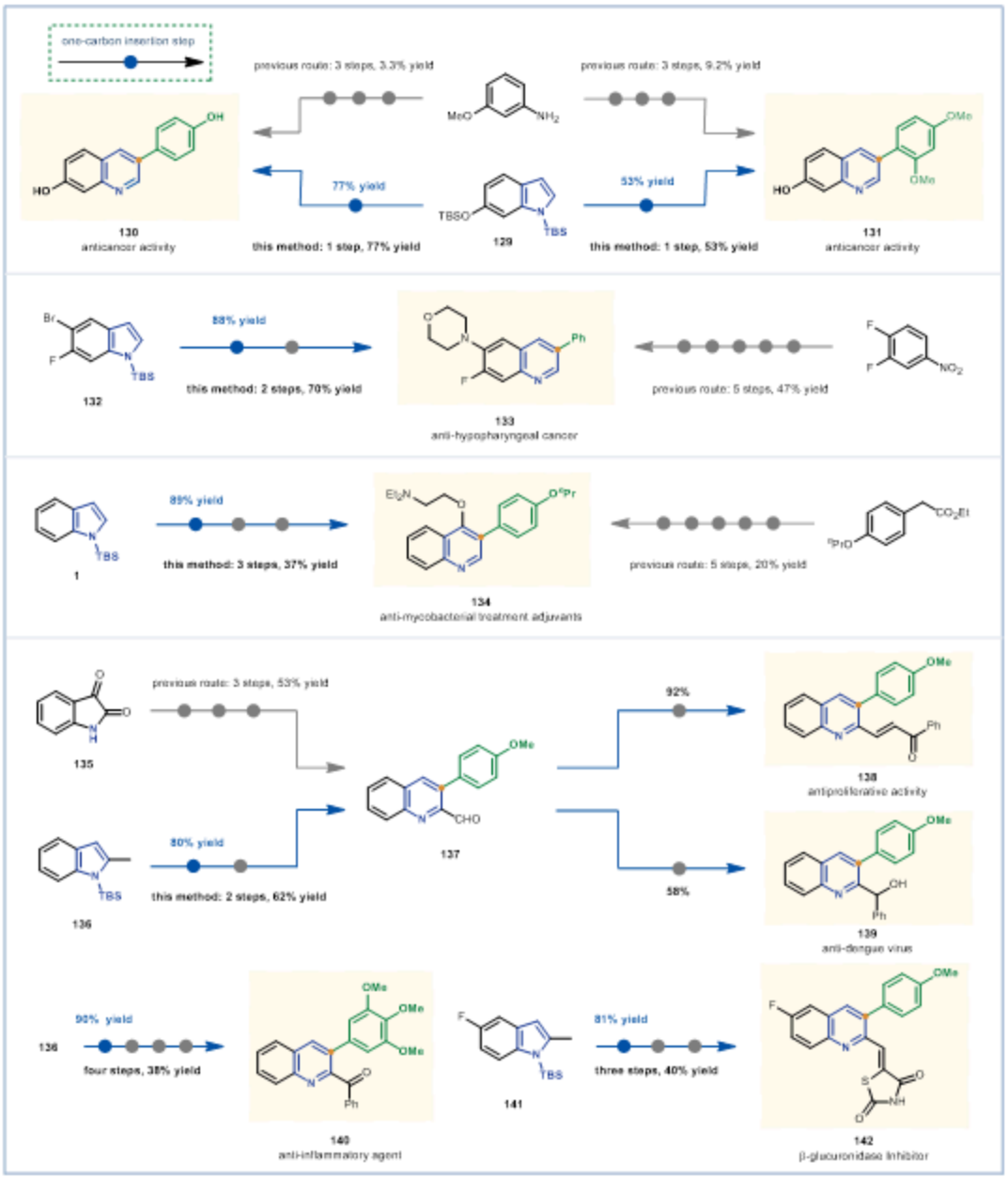

Figure 4

The synthetic utility of the halogen-free Ciamician-Dennstedt reaction in total synthesis of bioactive molecules.

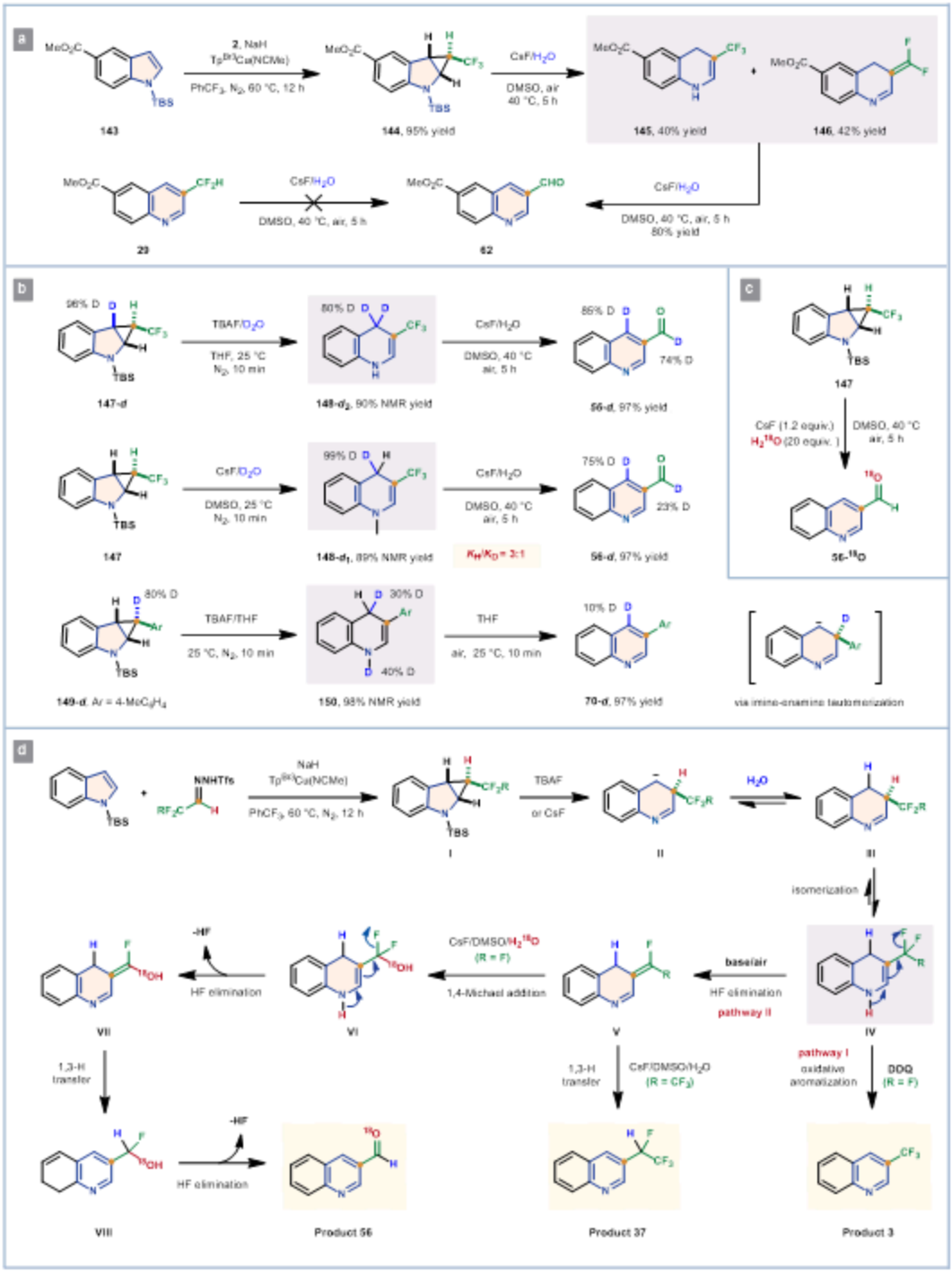

Figure 5

Mechanistic studies of carbon-atom insertion of indoles with fluoroalkyl carbenes. a,Identification of the reaction intermediates. **b,** Experiments to probe the source of the hydrogen atom incorporated in quinoline-3-carboxaldehyde. **c,**Probing source of oxygen atom incorporated into quinoline-3-carboxaldehydes. **d,**Proposed mechanistic pathways for direct, hydrodefluorinative, or defluorinative carbonylation carbon-atom insertion of fluoroalkyl carbenes into indoles.

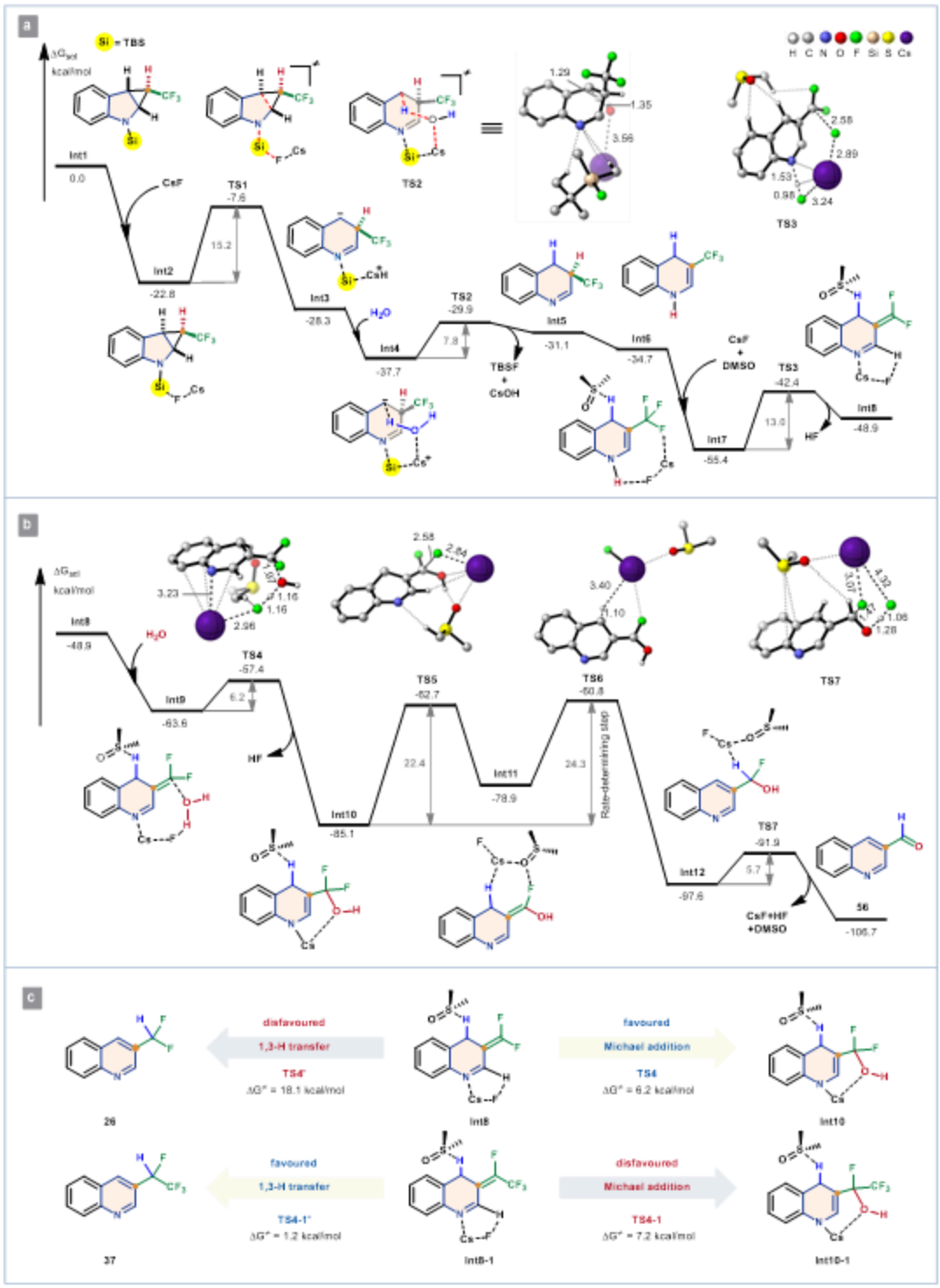

Figure 6

Computational studies. a, Calculation of *gem*-difluoromethylene intermediate **Int8** formation. **b,** Calculation of CsF-assisted 1,3-H transfer of intermediate **Int8** leading to quinoline-3-carboxaldehyde **56**. **c,** Investigations into the origin of chemoselectivity between CF_3- and CF_2CF_3-substituted *N*-triftosylhydrazones. Calculations were carried out at the SMD(DMSO)-M06/6-31G(d,p)-SDD(Cs) level of theory. Energies are in kcal/mol. Distances are in ångstroms. Most hydrogen atoms in 3D structures are omitted for clarity.

Supplementary Files

This is a list of supplementary files associated with this preprint. Click to download.

- SupplementaryDatacalculationsarchive.docx
- SupplementaryInformation.docx